Korean Journal of Chemical Engineering
https://doi.org/10.1007/s11814-024-00179-1

REVIEW ARTICLE (INVITED ONLY)

Recent Developments in Quantum Dot Light-Emitting Diodes for Skin-Attachable Electronics

Kiwook Kim[1] · Minseo Kim[1] · Jiwoong Yang[1,2]

Received: 16 March 2024 / Revised: 16 March 2024 / Accepted: 23 April 2024

Abstract
Recent advances in skin-attachable electronics have attracted substantial interest because of their potential in various fields such as robotics, healthcare, and wearable technology. Among various electroluminescent (EL) devices, quantum dot light-emitting diodes (QLEDs) are promising for next-generation displays due to their superior color purity, high brightness, excellent efficiency, high stability, and ultrathin form factors, making them promising for flexible electronic applications. This review outlines the recent progresses in QLEDs for skin-attachable electronics. First, materials selection and various structural designs that impart mechanical flexibility into QLEDs are discussed. We also discussed the design strategies of flexible displays based on the array of QLEDs. Then, we summarize skin-attachable displays based on the flexible QLEDs, including the integration with sensors capable of detecting various signals. The discussion includes the promising role of skin-attachable QLEDs in healthcare, particularly their potential as wearable light sources for monitoring biologic signals. Overall, this review article highlights the remarkable progress made in the skin-attachable QLEDs.

Keywords Quantum dot · Light-emitting diode · Skin-attachable electronics · Electroluminescence

Introduction

Displays, as luminescent devices, play a crucial role in visualizing external signals—environmental, electrical, or optical—and conveying information to users [1–3]. To deliver more realistic information, the development of displays has focused on enhancing key parameters related to the visualization, including brightness, color purity, and resolution. This trend has led to the exploration and utilization of various light-emitting materials with enhanced optical properties. Among these, quantum dots (QDs) have been emerging as next-generation light-emitting semiconductor materials, offering substantial advantages for display device applications [4–8]. QDs possess exceptional optical properties such as easily tunable bandgap, high photoluminescence quantum yield (PLQY), and high color purity with narrow emission spectra [9–15]. Quantum dots light-emitting diodes (QLEDs), which utilize the electroluminescence (EL) of QDs, exhibit high color purity, low turn-on voltage, high external quantum efficiency (EQE), and high brightness due to the outstanding optoelectronic properties of QDs [7, 16–24].

Concurrently, there has been growing demand for display devices that can be directly attached to the skin and can visualize immediate physical, optical, and electrical information [25–27]. Such displays are essential for the advancement of various future technologies such as robotics, healthcare, and wearable technology [28–33]. Traditional attempts to incorporate such devices into wearable forms, like glasses or watches, have faced challenges due to their rigid, thick, and fixed structures, leading to user discomfort during various activities. Consequently, there is a clear need for devices that can be conformably attached to the skin, integrating displays, sensors, and light sources for efficient biomedical detection. Because of the ultrathin thickness of active layers, QLEDs can be fabricated into ultrathin device structures [34]. When engineered for flexibility and stretchability, these ultrathin devices can significantly enhance portability, durability, and comfort during wear, adapting seamlessly to body

✉ Jiwoong Yang
jiwoongyang@dgist.ac.kr

[1] Department of Energy Science and Engineering, Daegu Gyeongbuk Institute of Science and Technology (DGIST), Daegu 42988, Republic of Korea

[2] Energy Science and Engineering Research Center, Daegu Gyeongbuk Institute of Science and Technology (DGIST), Daegu 42988, Republic of Korea

Published online: 10 May 2024

movements. Integrating QLEDs with sensors, light sources, and bio-signal detectors can result in a skin-attachable display-sensor system.

In this review article, we provide a comprehensive summary of the latest advancements in skin-attachable QLEDs (Fig. 1). The first chapter summarizes the fabrication strategies of flexible QLEDs. We discuss the use of flexible electrodes and structural designs (ultrathin, kirigami, wrinkled structures, etc.) to achieve skin compatibility for flexible QLEDs. The development of flexible displays based on QLED arrays is also summarized. The second chapter introduces a range of skin-attachable systems that integrate sensor-QLED displays. These systems have been successfully demonstrated to effectively transmit a wide range of signals, such as pressure, temperature, light, and strain. Beyond strategies for simple signal transmission, we also showcase interactive QLED displays capable of instantaneously conveying quantitative and spatial information in real-time. Furthermore, we present the applications of QLEDs as light sources in healthcare applications.

Design Strategies for Flexible QLEDs and Displays

When skin-attachable electronic devices are utilized, they are subjected to various mechanical deformations due to body movements. A crucial aspect of this development is the design of devices that are robust to mechanical damage resulting from such deformations. This chapter begins by discussing the selection of flexible materials for key components of flexible QLEDs, such as electrodes and substrates. The strategic choice of materials inherently imparts a degree of flexibility to QLEDs, enabling them to adapt to physical stresses. Beyond the selection of materials, this chapter also present another critical strategy: the structural modifications of QLEDs. This approach focuses on designing the QLED structure to ensure that functionality and integrity are maintained under physical distortions, such as twisting, bending, or stretching. Finally, to convey information effectively, displays requires more than just a single QLED and need to be composed of arrays containing multiple QLED

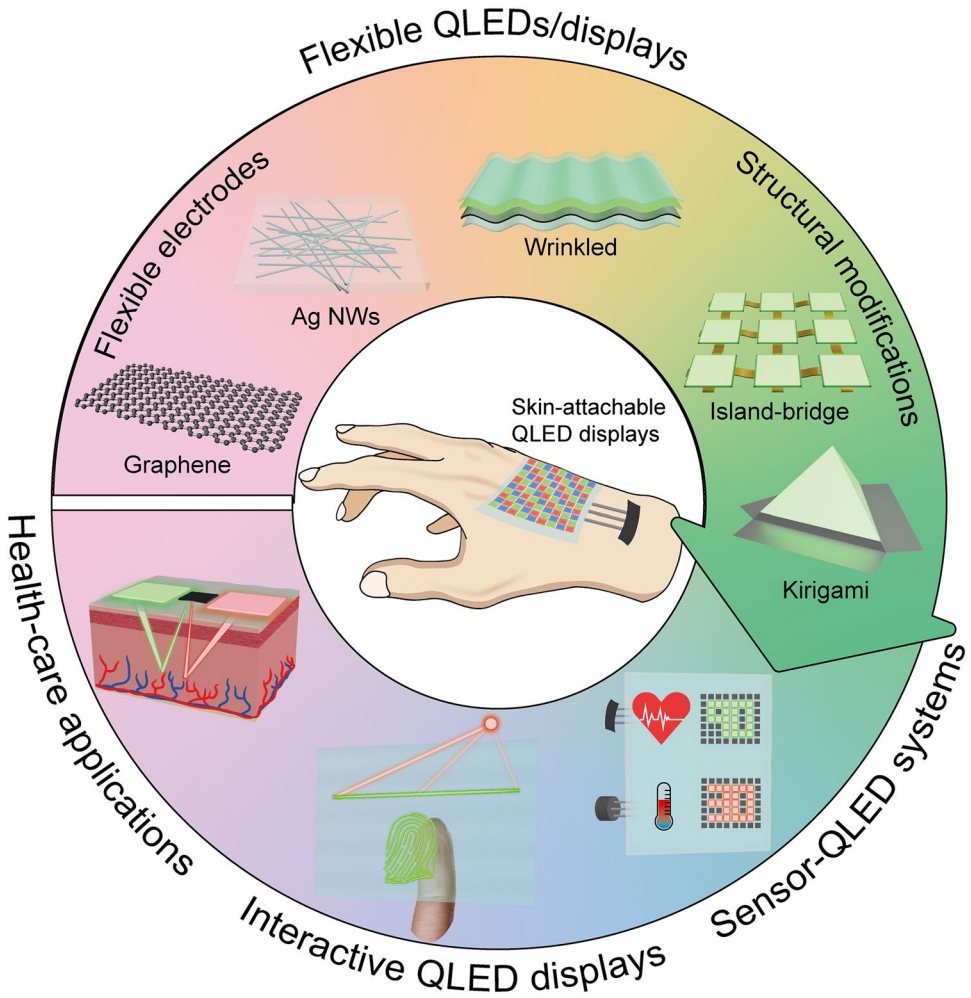

Fig. 1 Schematic overview on the developments of skin-attachable QLEDs

pixels. Therefore, this chapter concludes by highlighting representative works that showcase flexible displays based on arrays of QLEDs.

QLEDs with Flexible Electrodes

The use of flexible substrates has been explored to achieve mechanical properties suitable for flexible devices [35–39]. For instance, Yang et al. proposed highly stable QLEDs that can function like stickers, utilizing the Kapton polyimide (PI) substrates [40]. This substrate shows remarkable stability against many organic solvents and high temperatures (> 260 °C) [41–44], enabling stable adhesion on surfaces with varying curvatures. In addition to PI, various materials such as polycarbonate (PC), polyethylene naphthalate (PEN), polyethylene terephthalate (PET), epoxy, and poly(dimethylsiloxane) (PDMS) have been suggested as flexible substrates for flexible QLEDs [45–48]. However, when using plastic substrates alone, issues such as low moisture stability and low adhesion from differences in elasticity between the substrate and the electrode can affect device performance. To address this, strategies such as coating the substrate with materials like metal and colloidal nanoparticles have been suggested [49–51]. Using flexible substrates is essential in fabricating flexible devices, and various strategies are being suggested.

The flexibility of the electrode layer, an essential component in electronic devices, is also a critical consideration. While indium tin oxide (ITO) is known for its excellent electrical, mechanical, and optical properties, its brittleness and vulnerability to deformation pose challenges [52–55]. To incorporate the electrically superior yet brittle ITO layer in flexible devices, modifications of the electrode structure are required. Remarkably, mechanical neutral plane systems comprising metal layers sandwiched between two ITO layers (*e.g.*, ITO-copper-ITO structures, ICI) have been proposed [56–59]. These designs help disperse mechanical stress, protecting the ITO layer during bending tests [60, 61]. Song et al. further enhanced this concept with an epoxy-Cu-ITO (ECI) multilayer electrodes, improving transparency, conductivity, and flexibility compared to the standard ICI electrodes [62].

The inherent lack of mechanical deformability in ITO necessitates the development of alternative electrode materials with higher levels of deformation. Various materials, including carbon nanotubes (CNTs), graphene, and silver nanowires (AgNWs) have been suggested as transparent and flexible electrodes [63]. Choi et al. successfully developed flexible QLEDs using graphene as an anode, leveraging its transparency, flexibility, stretchability, and high electrical conductivity/mobility (Fig. 2a) [64]. The resulting device demonstrated high transparency (Fig. 2b), except in the semi-transparent Li/Al cathode section, and effective carrier injection, leading to high electrical/optical efficiency (Fig. 2c). These QLED devices maintained consistent performance during bending with the bending angle up to 180° (Fig. 2d).

As another alternative, dielectric/metal/dielectric (DMD)-based transparent electrodes have been emerging as promising candidates for electrodes of flexible electronic devices, because of their high conductivity, transparency, flexibility, and easy fabrication [65–67]. Kim et al. introduced flexible QLEDs based on oxide/metal/oxide (OMO) electrodes, a type of DMD electrode (Fig. 2e) [68]. Ag was chosen as the conducting metal, while WO_x and MoO_x were proposed as the dielectric metal oxide materials. The performance of the device was compared by controlling each material and the thickness of each layer (Fig. 2f and g). As the thickness of each oxide layer increased, the device performance decreased due to increased electrical resistance limiting electron injection into the electron transport layer (ETL). The devices with MoO_x as the oxide material outperformed those with WO_x, attributed to the energy levels relative to the ZnO layer used as an ETL. Remarkably, the device with MoO_x layer showed the better performance compared to those with ITO electrodes. Lee et al. also reported flexible QLEDs with a similar structure (Fig. 2h) [69].

AgNWs have been proposed as highly promising materials for flexible electrodes due to their excellent electrical, thermal, and mechanical properties [70]. Zhang et al. reported the application of AgNWs electrodes with a high transmittance of 98.5% in transparent QLEDs [71]. The use of AgNWs in combination with polymer composites, such as PI, has been suggested to offer higher deformability and reduced surface roughness and resistance [72]. Therefore, various studies have proposed to apply such composite materials in QLEDs. Ding et al. developed high-performance/high-efficiency QLEDs employing AgNW/PI electrodes [73]. In AgNW/PI structures, AgNWs effectively scatter trapped light into the air, reducing light reflection interfaces and thus increasing the amount of extracted light. AgNW electrodes have a lower work function than ITO anodes, suggesting more favorable electron injection into QDs (Fig. 2i). Devices using AgNW electrodes showed a higher EL intensity compared to those with ITO anodes at the same current level (Fig. 2j) and achieved excellent EQE of 24.1% (Fig. 2k). Moreover, these devices maintained electrical characteristics even after multiple bending tests, highlighting their flexibility and stability (Fig. 2l).

Ultrathin QLEDs with Structural Designs

The ultrathin structure of flexible electronic devices offers significant advantages, primarily because the stress induced by bending is directly proportional to the distance from the neutral axis [74, 75]. Furthermore, the ultrathin form factor

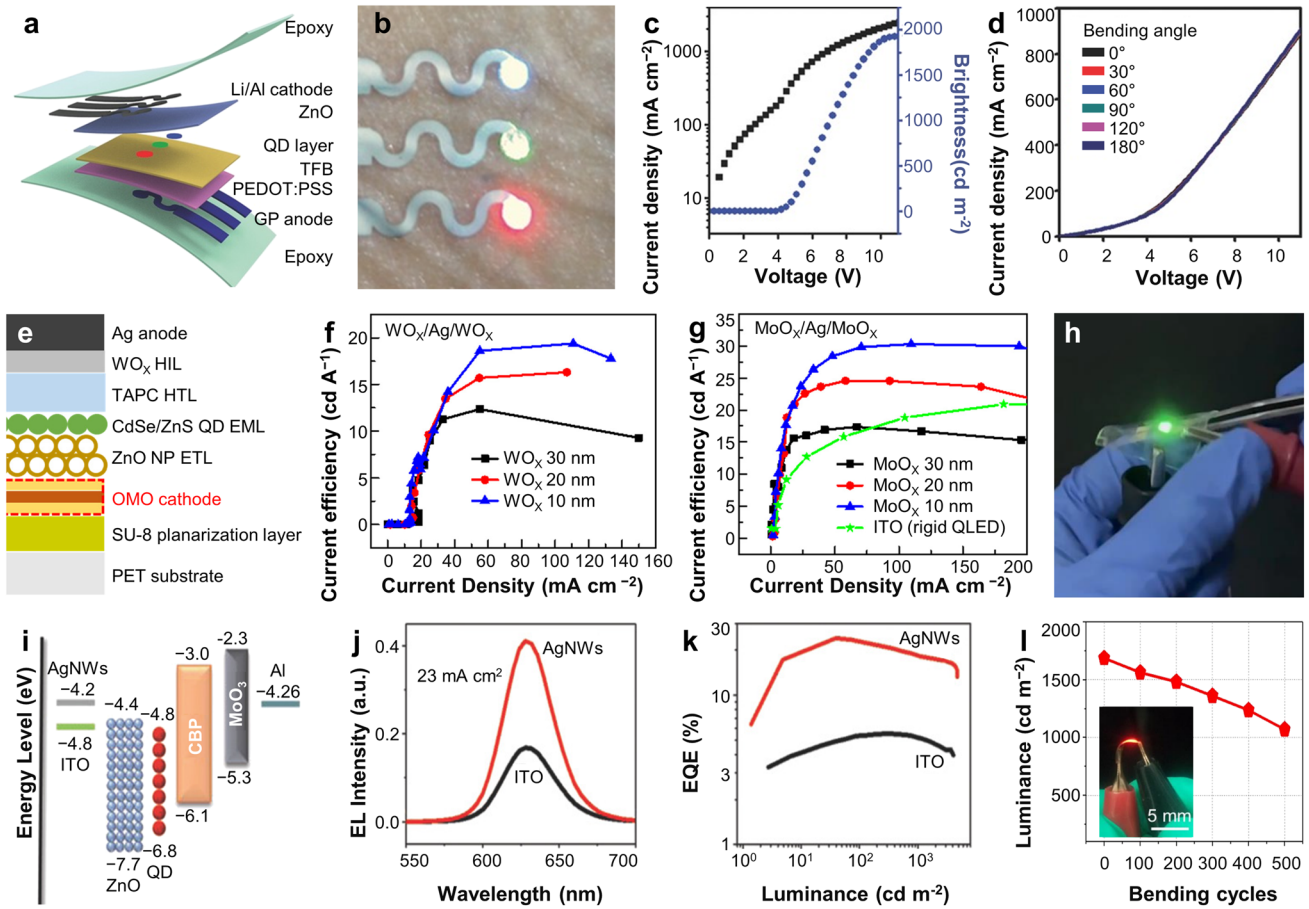

Fig. 2 **a** Schematic illustration of the device structure for wearable QLEDs with graphene anodes. **b** Photograph of the wearable QLED on the human arm. **c** Current density – brightness – voltage curves of the wearable QLED. **d** Current density – voltage curves of wearable QLEDs with various bending angles. Reproduced with permission from Ref. [64], Copyright 2015, WILEY–VCH. **e** Schematic illustration of QLEDs structure with OMO cathodes. **f** Current efficiency versus current density curves of QLEDs with various thickness of WO_x/Ag/WO_x and **g** MoO_x/Ag/MoO_x layers. Reproduced with permission from Ref. [68], Copyright 2022, MDPI. **h** Photograph of the flexible QLED with an OMO cathode. Reproduced with permission from Ref. [69], Copyright 2023, MDPI. **i** Energy-level diagrams of QLEDs employing AgNW cathodes or ITO cathodes. **j** EL spectra and **k** EQE curves of QLEDs with AgNW cathodes or ITO cathodes. **l** Bending test results of fabricated QLEDs with AgNW-based cathode. Reproduced with permission from Ref. [73], Copyright 2018, WILEY–VCH

is particularly beneficial in skin-attachable devices, where it minimizes user discomfort during body movements. On the other hand, these skin-attachable devices need to be robust against degradation and performance losses caused by factors such as sweat, ambient moisture, and heat. The superior water and air stability of QLEDs (compared to organic LEDs) allows for the use of significantly thinner encapsulation layers, enabling the development of ultrathin QLEDs [76, 77]. Choi et al. reported flexible and skin-attachable ultrathin QLEDs by employing 1.2 μm parylene-C/epoxy bilayers as both the top and bottom encapsulation layers [34]. This design achieved an ultrathin total thickness of 2.6 μm (Fig. 3a), while ensuring high mechanical stability under various deformations and exposure to moisture (Fig. 3b). Moreover, this work succeeded in generating pure white light emissions from skin-attachable pixelated white QLEDs (WQLEDs) (Fig. 3c). The efficiency and white color purity of the reported WQLEDs, featuring red/green/blue pixels, were superior to those of conventional WQLEDs. The traditional WQLEDs, which were fabricated by mixing various color of QDs within the light-emitting layer, frequently exhibit inefficiencies and reduced white purity, which is attributed to inevitable energy transfer between QDs of different colors [78].

QLEDs with an ultrathin form factor can benefit from additional structural modifications to allow the high degree of mechanical flexibility. One such modification is the incorporation of wrinkled structures, pre-engineered with wave-like patterns. These structures can flatten out under external tension, effectively releasing the deformation. The wrinkled

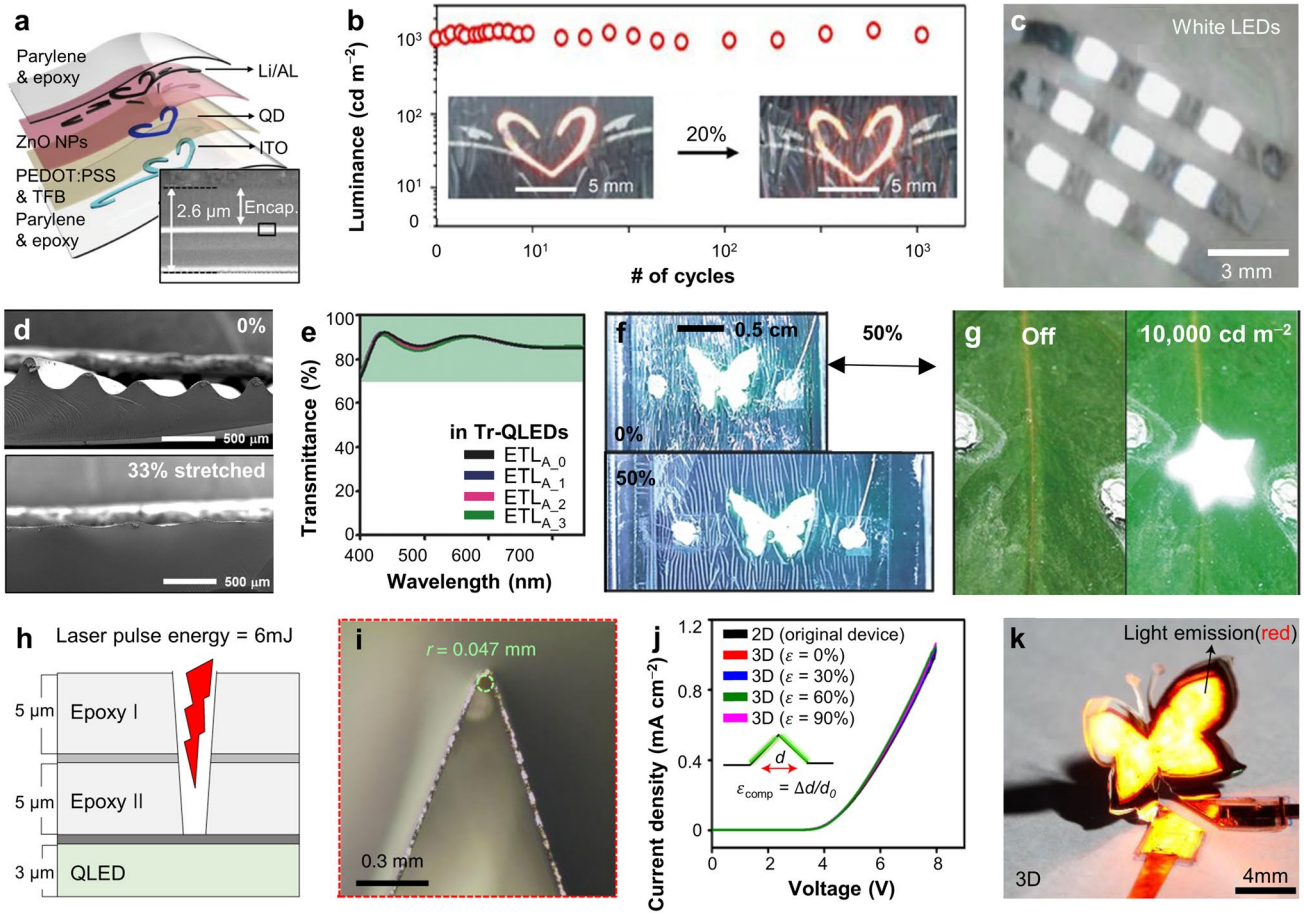

Fig. 3 **a** Schematic illustration showing the device structure of ultrathin QLEDs. **b** Brightness of the ultrathin QLEDs during stretching tests. **c** Photograph of skin-attachable WQLED arrays. Reproduced with permission from Ref. [34], Copyright 2015, Springer Nature. **d** Cross-sectional SEM image of wrinkled QLED structure under 0% and 33% stretching. **e** Transmittance spectra of QLEDs with the ETL_{A_x}, where x represents the thickness of alumina overlayers (nm). **f** Skin-attached QLEDs stretched up to 50%. **g** Photographs of QLEDs on leaves with varying luminance. Reproduced with permission from Ref. [79], Copyright 2018, WILEY–VCH. **h** Schematic illustration of etching strategies for kirigami designs and **i** photograph of the folded device. **j** Current density – voltage curves under various compressive strain. **k** Photograph of red-light-emitting QLED with a 3D butterfly structure. Reproduced with permission from Ref. [86], Copyright 2021, Springer Nature

structure applied for skin-attachable displays demonstrated high folding and tensile capabilities. Choi et al. proposed engineering strategies for flexible and transparent QLEDs using the wrinkled architecture (Fig. 3d) [79]. An ETL composed of ZnO nanoparticles deposited with ultrathin alumina overlayers enabled the use of ITO for both top and bottom electrodes, resulting in high transparency (≥ 84% transparency at the visible range) and superior EL performance (max luminance ≈ 73,000 cd/m^2 at 9V) (Fig. 3e). The ultrathin alumina overlayers not only effectively protected the underlayers during the top ITO electrode deposition but also enhanced the balance of the electron and hole injection into QDs. With the introduction of wrinkled structures, these devices exhibited a resilient folding structure even at very small bending radii. In addition, it maintained stable EL performance even in tensile tests with the strain up to 50% (Fig. 3f). As results, the reported QLEDs demonstrated outstanding transparency and clarity of visual data on color-rich backgrounds (such as leaves) (Fig. 3g).

Integrating origami and kirigami designs with QLEDs has opened new possibilities in overcoming the challenges regarding the creation of 3D architectures, paving the way for the next-generation displays that go beyond traditional curved form factors to more complex and versatile designs [80–84]. Prior to its applications to QLEDs, the concept of kirigami has been applied for OLEDs, showcasing the potential for various intricate 3D structures such as pop-up and candle-flame shapes [85]. Kim et al. made significant advances in the field of QLEDs by developing 3D foldable QLED devices. This was achieved through the device design using alloy-type etch-stop layers to precisely form cutting lines (Fig. 3h)

[86], resulting in foldable structures with very small bending radii. The cutting process of the encapsulation layer was precisely controlled by the employment of laser and etch-stop layer, ensuring that electrodes, charge transport layers, and light-emitting layer remained intact. As a result, folding in the desired regions of the EL device was easily achieved using the kirigami approach. The maximum bending radius of the device with two epoxy layers etched was found to be over 30 times smaller (~ 0.047 mm) than that of a device encapsulated with epoxy without etching, and at the same time, there was no degradation of electrical properties (Fig. 3i and j). Through this strategy, QLEDs of various 3D architectures, such as airplane, butterfly, and pyramid structure, were demonstrated (Fig. 3k).

Flexible Displays Based on the QLED Arrays

To effectively convey information, displays must be composed of arrays containing multiple pixels, rather than relying solely on a single LED. In this regard, Kim et al. developed ultrathin pixelated QLED displays based on the passive matrix array operation (Fig. 4a) [87]. This work utilized the design strategy similar to skin-attachable QLED reported by the same research group (Fig. 3a-c) [34], employing ultrathin parylene-C/epoxy double layers as the encapsulation layers. QLEDs with ultrathin ITO electrodes were arranged with pixelated islands within the encapsulation layers, resulting in ultrathin pixelated QLED displays with the total thickness of ~5.5 μm. This design could offer excellent waterproof properties even against direct droplet contact and prevent damage during intense and repeated crumpled deformation (Fig. 4b and c). This design was also beneficial

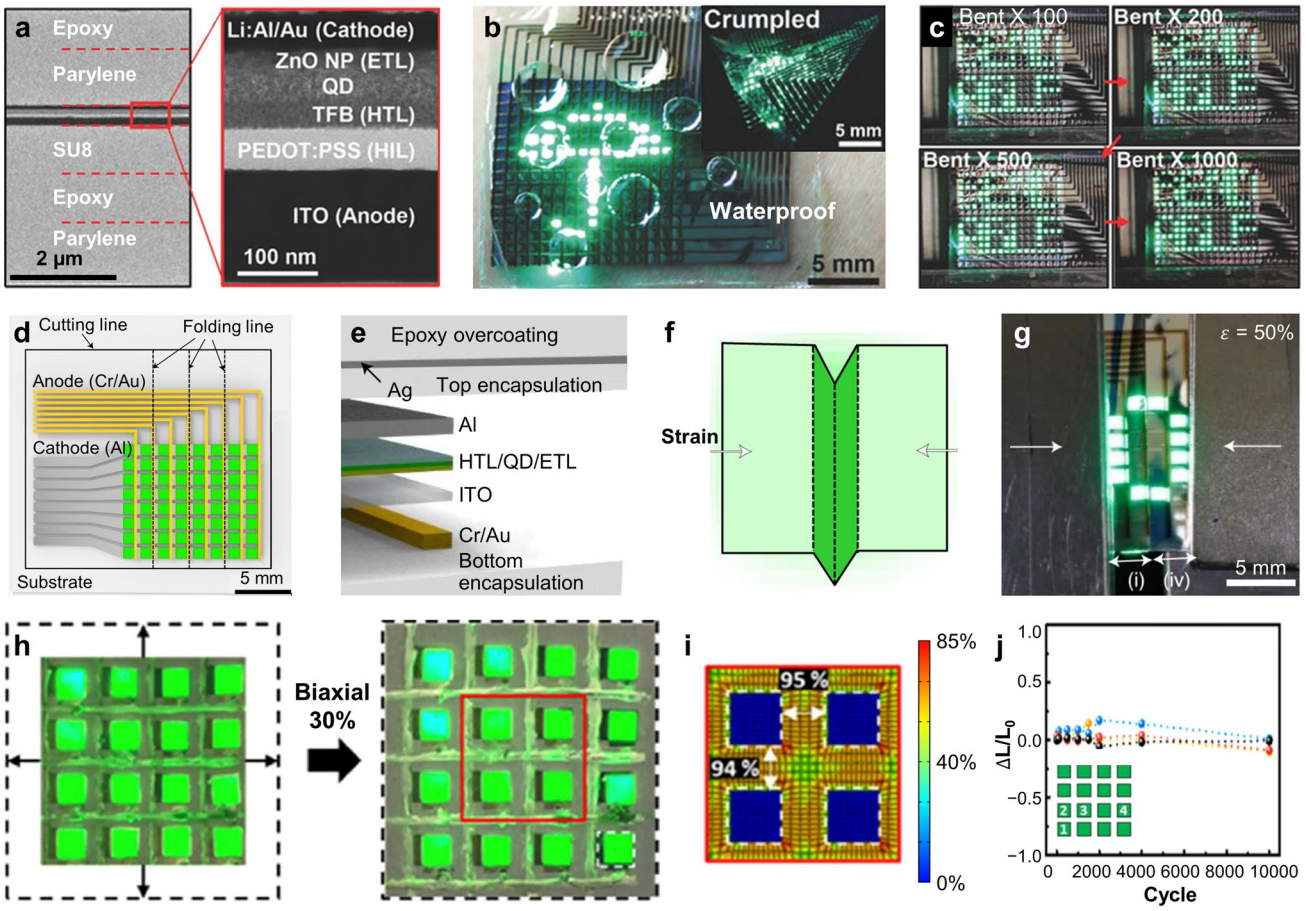

Fig. 4 **a** Cross-sectional TEM image of QLED display device and magnified TEM image from the red box. **b** Water-stability, crumpling, and **c** repetitive bending tests of 16×16 green QLED display. Reproduced with permission from Ref. [87], Copyright 2017, WILEY–VCH. **d** Schematic illustration showing pixelated QLED display with a pre-programmed folding line and **e** the device structure of 3D foldable QLED displays. **f** Schematic illustration of folding strategy and **g** photograph of QLED display. Reproduced with permission from Ref. [86], Copyright 2021, Springer Nature. **h** Photographs of the stretchable QLED array under the biaxial stretching test and **i** results of FEM analysis from red-box area. **j** The normalized EL-intensity changes of rigid QLED islands with the repetitive uniaxial stretching test. Reproduced with permission from Ref. [92], Copyright 2021, Elsevier

for conformal skin attachment. Consequently, with a passive matrix array, the ultrathin QLED displays (16 × 16 and 24 × 24) could visualize various patterns, including letters, numbers, and symbols, directly on human skin.

Utilizing kirigami techniques, ultrathin pixelated QLED displays show potential for transformation into a 3D form. Indeed, there are several reports in which kirigami designs have been successfully integrated into various pixelated electronic devices, suggesting its applicability to QLED displays [88–91]. Kim et al. demonstrated 3D foldable QLED displays utilizing a kirigami structure, achieved through the controlled etching of the encapsulation layer [86]. To prevent damage to each QLED pixel, folding lines were placed between the pixels (Fig. 4d and e), allowing for inward–outward folding with visualization of texts or images (Fig. 4f and g).

The island-bridge structure suggests another significant advancement in QLED-based display technologies. Pixels based on QLEDs act as "islands", which are electrically and mechanically connected by elastic materials as "bridges". This design minimizes the strain in the pixel areas during the stretching, preventing mechanical damage on QLEDs. Lee et al. reported flexible QLED displays based on QLED island arrays on Ecoflex/PDMS substrates [92]. Initially, QLED pixel arrays were fabricated on islands of Norland Optical Adhesive 63 (NOA63), which were arranged on a glass surface treated with an octadecyltrichlorosilane self-assembled monolayer (OTS-SAM). Subsequently, these arrays were transferred onto a stretchable Ecoflex/PDMS substrate. The electrical connection between arrays was achieved using liquid metal Galinstan, ensuring minimal deformation of the QLED pixels. To enhance the mechanical flexibility of the QLEDs during deformation, they employed flexible and transparent electrodes made of an Au grid combined with ethylene glycol-doped poly(3,4-ethylenedioxythiophene):poly(styrenesulfonate) (PEDOT:PSS) instead of conventional ITO electrodes [93, 94]. The proposed QLED displays could be stably attached to the skin, maintaining their performance without degradation even at uniaxial strain of 50% and biaxial strain of 30% (Fig. 4h). To assess the strain distribution, the finite element method (FEM) analysis was conducted, confirming that most of the strain was predominantly applied on the flexible substrates (Fig. 4i). In addition, the brightness of the QLED island pixel was maintained after deformation (Fig. 4j).

Flexible QLEDs for Skin-Attachable Electronics

For skin electronic systems, flexible displays are essential components for visualization of information, including signals detected by wearable sensors. While commercialized smartwatches, such as those from Apple (2015) and Samsung Electronics (2018), serve as representative examples of integrating wearable sensors with displays, their thickness and rigidity can limit versatility during various activities and cause discomfort during prolonged use. The flexible QLEDs discussed in the previous chapter are promising for skin-attachable electronics, because of their superior device characteristics during various mechanical deformations and ultrathin form factors. This chapter showcases the recent advancements in utilizing flexible QLEDs for skin-attachable electronic systems. We begin by exploring skin-attachable QLED displays that are integrated with wearable sensors. Following this, we introduce pioneering research that has utilized skin-attachable QLEDs as wearable light sources for biomedical applications, highlighting their unconventional roles in skin electronics.

Skin-Attachable QLED Displays Integrated with Wearable Sensors

Skin-attachable displays, when integrated with wearable sensors, provide a convenient and effective solution for visualizing signal for skin electronic systems [95–98]. Lee et al. reported stretchable QLED array-signal monitoring systems (Fig. 5a) [92]. Fabricated on an Ecoflex/PDMS substrate, the integrated QLED array and sensor exhibit stable performance under various mechanical deformations. Through the passive matrix operataion, the QLED displays could visualize the information from signals detected by the sensor [99, 100]. Specifically, in this study, a resistance-based stretchable strain sensor was employed to detect the strain changes induced by the body motion. This change was then read by a microcontroller unit (MCU), which drives the QLED array to display the strain as a specific pattern. This system allowed for immediate visual representation of the strain (Fig. 5b and c).

The advancement of QLED displays that are integrated with sensors extends to the transduction of various signals into visual information. This includes the continuous monitoring of external environment. For instance, Lee et al. added an external environment sensing system to devices which have similar structure with above (Fig. 5d) [101]. The system included various sensors for a wide range of signals (Fig. 5e): i) the UV sensor made of ZnO NW/CNT, showing changes in the resistance upon UV irradiation, and a temperature sensor composed of CNT/polyaniline (PAni), leading the resistance decrease with the temperature increase. These changes in resistance were then visualized on the QLED displays (Fig. 5f).

Furthermore, Kim et al. introduced stretchable sensory-neuromorphic systems (SSNSs) that integrate a pressure sensor with a QLED display for detecting and visualizing patterned pressure (Fig. 5g) [102]. The system included

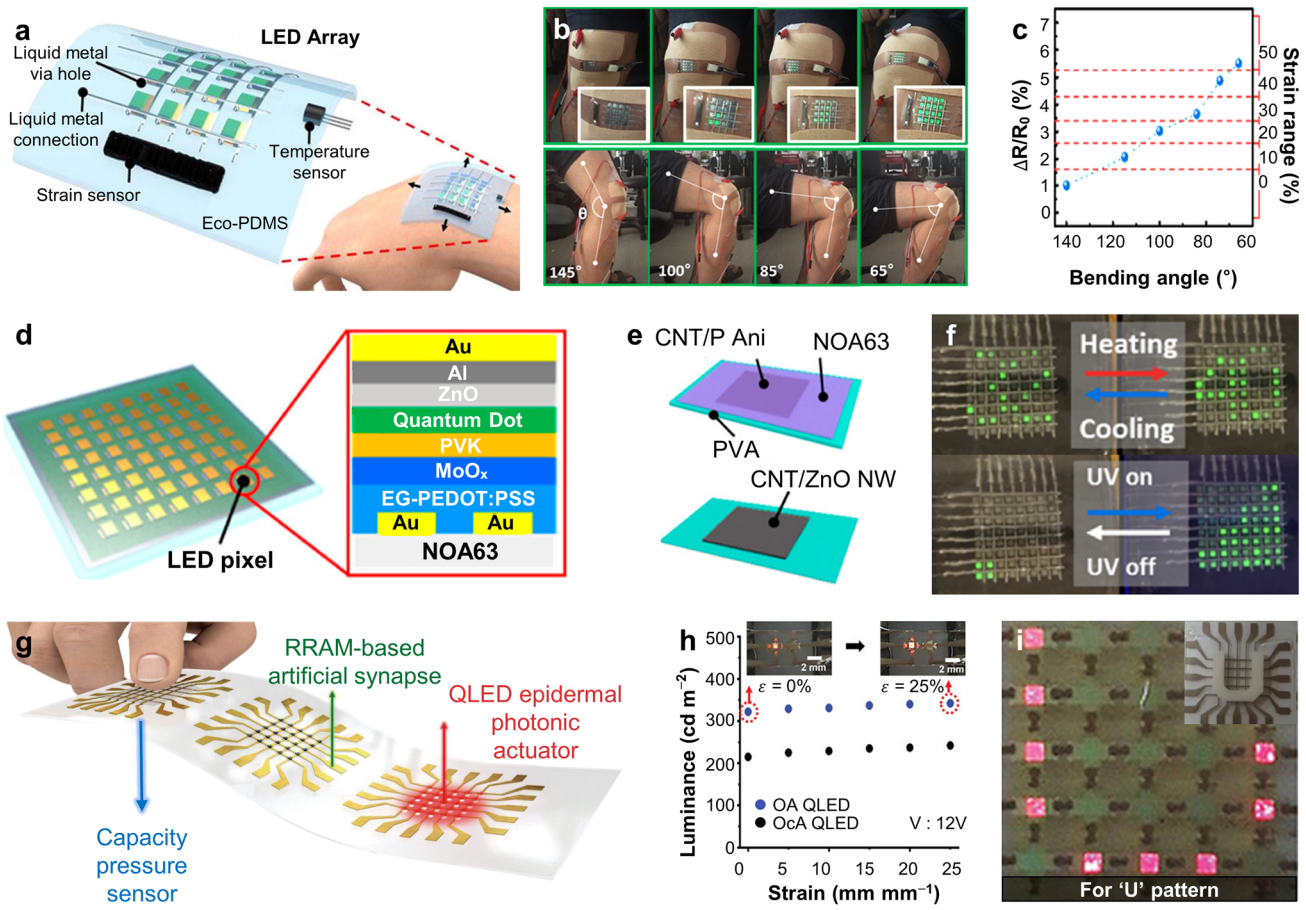

Fig. 5 **a** Schematic illustration of strain sensor-QLED integrated device. **b** Patterns of QLED display corresponding to the applied strain from various knee bending angles. **c** Normalized resistance changes and strain range in relation to bending angles. Reproduced with permission from Ref. [92], Copyright 2021, Elsevier. **d** Schematic illustration showing the device structure of pixelated QLED arrays. **e** Schematic illustration of temperature sensor (top) and UV sensor (bottom) structure. **f** Visualization of temperature (top) and UV irradiation (bottom) by QLED displays. Reproduced with permission from Ref. [101], Copyright 2022, American Chemical Society. **g** Schematic illustration of stretchable sensory-neuromorphic system. **h** Changes in luminance of QLED pixels under various strains. **i** Photographs of pressing the sensor with a "U" pattern and the corresponding QLED display visualizing pattern. Reproduced with permission from Ref. [102], Copyright 2021, WILEY–VCH

a capacitive pressure sensor as an artificial mechanoreceptor, which can process external pressure into electrical potential. Then, this data was trained and inferred in resistive random-access memory (RRAM) using a back-propagation algorithm, and finally visualized through QLED-based epidermal photonic actuators. For stretchablity, QLED pixel islands were placed on the PDMS substrate. This design enabled high mechanical stability under skin deformations up to 25%, without changes in the luminance of each QLED pixel (Fig. 5h). Operational tests showed that the SSNS could successfully translate various stimuli into image patterns (Fig. 5i), using a stable artificial conversion program to ensure consistent data processing and accurate pattern recognition, even under deformation.

Interactive Sensing Displays Based on QLEDs

The above systems that combine QLED displays with sensors primarily function by converting sensor signals into visual information on the displays. Recent developments have led to the creation of devices that can concurrently serve as sensors and light-emitting diodes, showing great promise for interactive sensing displays. These dual-function technologies offer significant advantages, including an extensive range of flexibility in device design and the ability for instantaneous communication of spatiotemporal information, as they eliminate the need for a separate signal conversion process between the display and the sensor.

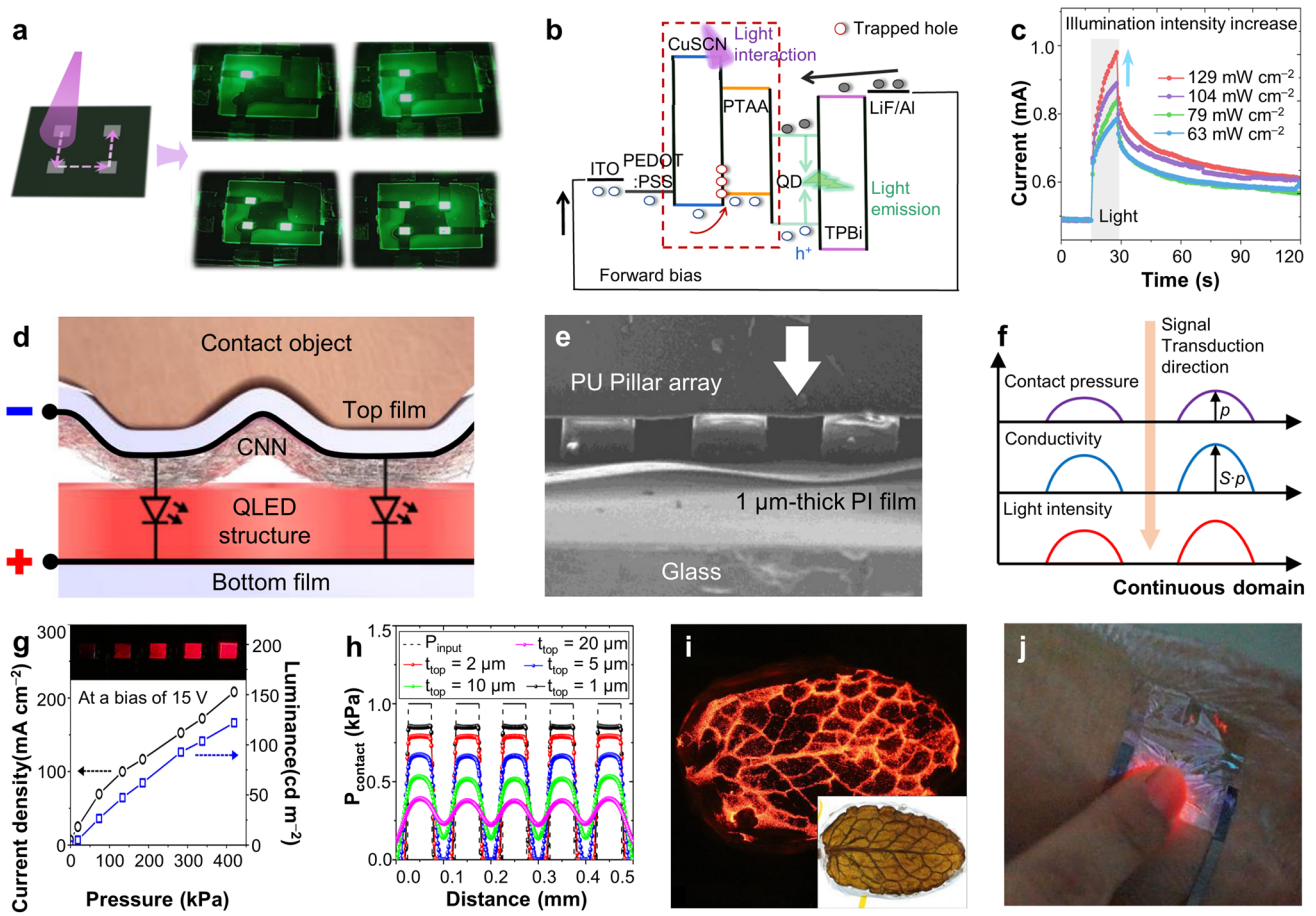

Fig. 6 **a** Schematic illustration of the light-sensing process and photographs of QLED devices. **b** Energy-level diagram and operating mechanism of light-sensing interactive QLEDs. **c** Current versus time curves of interactive QLED under the light irradiation with different intensities. Reproduced with permission from Ref. [103], Copyright 2022, Springer Nature. **d** Schematic illustration of the skin-attachable pressure-sensing interactive QLED device. **e** Cross-sectional SEM image of an interactive QLED. **f** Distribution of contact pressure, conductivity, and light intensity induced by signal transduction. **g** Current density and luminance depending on the applied pressure under a bias of 15 V. **h** FEA simulation of contact pressure along to thickness of top film. **i** Photographs of visualizing the pressure applied with a leaf and **j** finger on the skin-attachable device. Reproduced with permission from Ref. [104], Copyright 2020, Springer Nature

Ju et al. reported light-sensing perovskite QLEDs (PQLEDs), suggesting their potential in interactive display applications [103]. Figure 6a presents a schematic illustration of a 2 × 2 light-sensing PQLED array and the actual experimental result. The underlying mechanism involves a photosensitive poly(bis(4-phenyl)(2,4,6-trimethylphenyl) amine) (PTAA) layer within the device structure, which absorbs external light signals to generate electron–hole pairs. These pairs are modulated within a copper thiocyanate (CuSCN)/PTAA bilayer, leading to increased current and EL in the PQLEDs (Fig. 6b). The intensity of the light signal can control carrier generation, thereby modulating the device current in response to varying light signal strengths (Fig. 6c).

The concept of dual-function devices is broadening to include the sensing of various signals. Lee et al. developed ultrathin (~3 μm) skin-attachable pressure-sensing interactive QLED systems, capable of visualizing spatiotemporal information in real-time [104]. In this device, the cellulose/nanowire nanohybrid network (CNN) which was coated on the top film played an essential role. Upon the application of pressure, the CNN came into contact with ETL of the QLEDs, triggering a piezoresistive effect (Fig. 6d and e). This effect created the direct relationship between the applied pressure, the conductivity, and the intensity of the EL from QLEDs (Fig. 6f), allowing for the visualization of pressure intensity through the brightness (Fig. 6g). Moreover, the thickness of semi-transparent cathode film/CNN double layer (~60% at the visible range for ~1 μm thick) significantly affected the sensitivity of pressure-sensing (Fig. 6h). At an optimal thickness of 1 μm, the device achieved remarkable sensitivity (> 5000 k/Pa) across a broad

area. These pixel-less structures can generate high-resolution EL images, corresponding to the conventional image with high pixel density (> 1000 dpi). As these images bypassed the analog-to-digital conversion process, the device exhibited the rapid response times (< 1 ms). This ultrathin/high transparency pressure-sensing interactive QLED device has successfully demonstrated high quality images of fine textures like the surface of leaves or fingerprints (Fig. 6i and j).

QLEDs as Wearable Light Sources for Healthcare Applications

The excellent optical properties of QLEDs can extend their utility beyond information display technologies to skin-attachable light sources for wearable healthcare applications, particularly in phototherapy and diagnosis [105]. Chen et al. demonstrated the potential of QLED light sources in stimulating cellular metabolisms and inducing cell destruction through photodynamic therapy at an in vitro level [106]. The narrow emission spectrum and high brightness of QLEDs could contribute as key factors for targeted phototherapy. Such findings hold promise for future wearable healthcare technologies using skin-attachable QLEDs.

In parallel, the development of skin-attachable photodiagnosis technology is essential in realizing real-time healthcare monitoring systems [107]. For example, photoplethysmogram (PPG) sensors are capable of non-invasively estimating heart rates, blood oxygen saturation (S_pO_2), and glucose levels [108–110]. These sensors operate by optically detecting changes in light absorption due to blood-volume variations in tissue microvascular beds. The safety and convenience of these sensors make them highly promising in wearable healthcare monitoring. There have been some reports utilizing skin-attachable QLEDs as light sources for PPG signal detection. For instance, Kim et al. developed transmission PPG sensors integrating wrinkled-structured QLEDs and QD-photodetectors (PDs) (Fig. 7a) [111]. This PPG sensor, designed with the QLED and the PD positioned at opposite ends of a fingertip, operated by detecting the light emitted from the QLED after it has transmitted through the fingertip [112]. The structural flexibility facilitated the creation of stable skin-attachable QLED light sources and PDs, capable of stretching up to 70 and 40%, respectively. This ensures stable operation and conformal contact of these devices even on small body structures like fingertips (Fig. 7b and c). The bright light from QLEDs, which were firmly attached on the skin, passed through the fingers with minimal leakage, enabling the PD to capture clear PPG signals (Fig. 7d and e). This integrated system, which has shown potential for application on various body parts and maintained high stability even in underwater environments, suggest the significant promise of the skin-attachable PPG sensors (Fig. 7f).

In another notable study, Lee et al. developed fiber-based QD pulse oximetry (FQPO) devices, suitable for integration into wearable clothing (Fig. 7g) [113]. To fabricate flexible, fiber-based QLEDs (FQLEDs), a flexible and transparent PET substrate, along with a PEDOT:PSS electrode, was used. An encapsulation layer, a 20 μm sandwiched structure composed of a silica (SiO_2) composite polymer and an alumina/zinc oxide (Al_2O_3/ZnO), was utilized to passivate the QD layer. FQLEDs constructed with this structure demonstrated high moisture stability and flexibility. These reflection-type PPG sensors detected the light reflected by the blood vessels using PDs [114, 115] This device employs both red and green light sources to measure pulse oximetry, optimizing for the differing absorption properties of oxyhemoglobin and deoxyhemoglobin (Fig. 7h). The narrow emission spectra of QLED light sources in this reflective measurement system addressed the challenges of variable detection values due to angle changes and minimized noise because of uniform Lambertian characteristics of QLEDs (Fig. 7i and j).

Conclusion

In this review, we provide a comprehensive overview of the cutting-edge development of in the field of skin-attachable QLEDs. QDs have gained considerable interest as promising materials for display technologies due to their exceptional optical and electrical properties. Various flexible QLED designs have been proposed, demonstrating their ability to retain EL characteristics under various mechanical deformations. These advancements have been realized through the synergistic combination of material selection and structural modifications, leading to the successful demonstration of a range of skin-attachable QLED devices, ranging from individual LEDs to displays comprising QLED arrays. Moreover, the integration of flexible QLEDs with wearable sensors opens new possibilities in skin electronics. These integrated systems can instantaneously visualize a broad spectrum of sensor-detected signals. Beyond conventional display-sensor integration, the concept of interactive sensing displays using QLEDs has been introduced. In addition, flexible QLEDs show significant promise as light sources in wearable healthcare applications, further broadening their range of possible applications.

While significant progress has been made, there are still notable challenges to overcome for the practical application of these technologies. One of the primary concerns is the limited mechanical stretchability of the currently developed QLEDs, primarily due to the use of materials lacking intrinsic stretchability. Future research needs to develop all component layers—such as substrates, electrodes, charge transport layers, and light-emitting layers—to be intrinsically

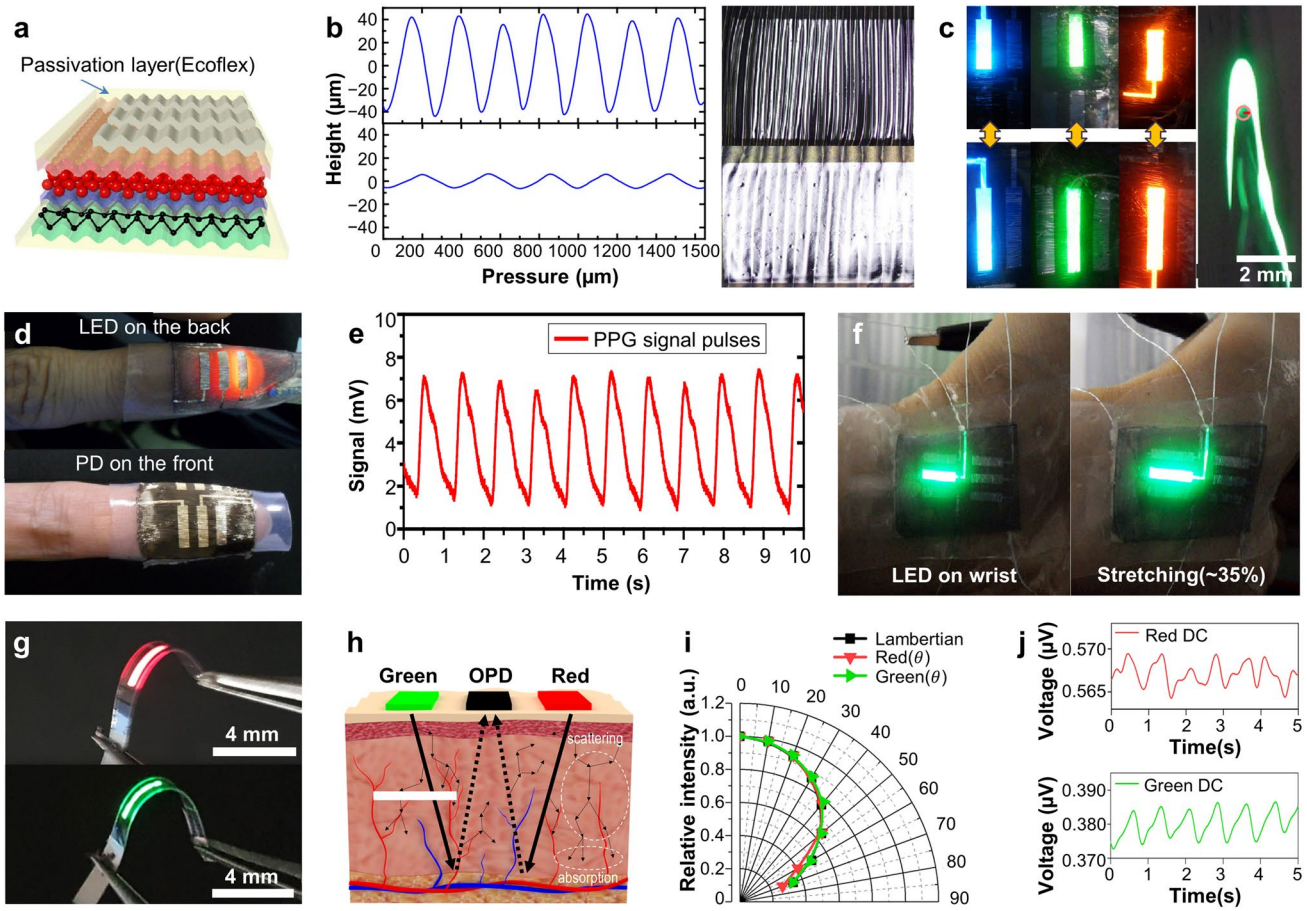

Fig. 7 **a** Schematic illustration of QLEDs with the wrinkled structure. **b** Surface profile (left) and photograph (right) of the wrinkled QLED with 20% strain (top) and 70% strain (bottom). **c** Photographs of the stretched red, green, and blue QLEDs under 0% strain (left top), 70% strain (left bottom) and bending deformation (right). **d** Skin-attached PPG sensor consisted with QLEDs and PDs. **e** Real-time PPG signal detected from a skin-attachable PPG sensor. **f** Photographs of stretched QLEDs attached on the wrist. Reproduced with permission from Ref. [111], Copyright 2017, American Chemical Society. **g** Photographs of red (top) and green (bottom) FQLEDs. h Schematic illustration of the operating principle of skin-attached FQPO devices. **i** Relative EL intensity of red and green FQLEDs with Lambertian characteristics according to angle. **j** PPG signal detected from FQPO devices attached at the finger. Reproduced with permission from Ref. [113], Copyright 2023, Springer Nature

stretchable [116–121]. Another major issue is the toxicity of QDs used in these devices, as many of them currently contain toxic elements like cadmium or lead. To achieve widespread commercialization and comply with regulations such as the Restriction of Hazardous Substances Directive (RoHS), the development of flexible QLEDs based on heavy-metal-free QDs is essential [122–129]. In addition, the operational stability of flexible QLEDs currently lags behind that of their conventional rigid counterparts. This gap highlights the need for a more comprehensive understanding of QD degradation mechanisms [130–133]. Lastly, the advancement of high-resolution QD printing techniques for flexible QLEDs is crucial [134–141]. These techniques must be compatible with the flexible QLED fabrication processes to achieve the excellent EL characteristics, realizing the full potential of skin-attachable QLED technologies.

Acknowledgements This work was supported by the National Research Foundation of Korea (NRF) grant funded by the Korean government (MSIT) (grant no. 2021R1C1C1007844). This research was also financially supported by the Ministry of Trade, Industry and Energy (MOTIE) and Korea Institute for Advancement of Technology (KIAT) through the International Cooperative R&D program (P0026257).

Data availability This review paper does not include experimental data generated by the authors. Thus, data sharing is not applicable.

References

1. H.E. Lee, J.H. Shin, J.H. Park, S.K. Hong, S.H. Park, S.H. Lee, J.H. Lee, I.S. Kang, K.J. Lee, Adv. Funct. Mater. **29**, 1808075 (2019). https://doi.org/10.1002/adfm.201808075

2. T. Sekitani, H. Nakajima, H. Maeda, T. Fukushima, T. Aida, K. Hata, T. Someya, Nat. Mater. **8**, 494 (2009). https://doi.org/10.1038/nmat2459
3. J. Yoo, S. Li, D.-H. Kim, J. Yang, M.K. Choi, Nanoscale Horizons **7**, 801 (2022). https://doi.org/10.1039/d2nh00158f
4. Z. Liu, C.H. Lin, B.R. Hyun, C.W. Sher, Z. Lv, B. Luo, F. Jiang, T. Wu, C.H. Ho, H.C. Kuo, J.H. He, Light Sci. Appl. **9**, 83 (2020). https://doi.org/10.1038/s41377-020-0268-1
5. J. Kim, J. Roh, M. Park, C. Lee, Adv. Mater. (2023). https://doi.org/10.1002/adma.202212220
6. E. Jang, S. Jun, H. Jang, J. Lim, B. Kim, Y. Kim, Adv. Mater. **22**, 3076 (2010). https://doi.org/10.1002/adma.201000525
7. J. Yang, M.K. Choi, U.J. Yang, S.Y. Kim, Y.S. Kim, J.H. Kim, D.-H. Kim, T. Hyeon, Nano Lett. **21**, 26 (2021). https://doi.org/10.1021/acs.nanolett.0c03939
8. M.K. Choi, J. Yang, T. Hyeon, D.-H. Kim, npj Flex Electron. **2**, 10 (2018). https://doi.org/10.1038/s41528-018-0023-3
9. C.B. Murray, D.J. Norris, M.G. Bawendi, J. Am. Chem. Soc. **115**, 8706 (1993). https://doi.org/10.1021/ja00072a025
10. Y. Shirasaki, G.J. Supran, M.G. Bawendi, V. Bulović, Nat. Photonics **7**, 13 (2013). https://doi.org/10.1038/nphoton.2012.328
11. J. Lee, J. Yang, S.G. Kwon, T. Hyeon, Nat. Rev. Mater. **1**, 16034 (2016). https://doi.org/10.1038/natrevmats.2016.34
12. H. Moon, C. Lee, W. Lee, J. Kim, H. Chae, Adv. Mater. **31**, 1804294 (2019). https://doi.org/10.1002/adma.201804294
13. J. Yang, F. Muckel, W. Baek, R. Fainblat, H. Chang, G. Bacher, T. Hyeon, J. Am. Chem. Soc. **139**, 6761 (2017). https://doi.org/10.1021/jacs.7b02953
14. F.P. Garcia de Arquer, D.V. Talapin, V.I. Klimov, Y. Arakawa, M. Bayer, E.H. Sargent, Science **373**, 8541 (2021). https://doi.org/10.1126/science.aaz8541
15. H. Kim, A. Choe, S.B. Ha, G.M. Narejo, S.W. Koo, J.S. Han, W. Chung, J.-Y. Kim, J. Yang, S.-I. In, Chemsuschem **16**, e202201925 (2023). https://doi.org/10.1002/cssc.202201925
16. S. Coe, W.K. Woo, M. Bawendi, V. Bulović, Nature **420**, 800 (2002). https://doi.org/10.1038/nature01217
17. K.S. Cho, E.K. Lee, W.J. Joo, E. Jang, T.H. Kim, S.J. Lee, S.J. Kwon, J.Y. Han, B.K. Kim, B.L. Choi, J.M. Kim, Nat. Photonics **3**, 341 (2009). https://doi.org/10.1038/nphoton.2009.92
18. Y.H. Won, O. Cho, T. Kim, D.Y. Chung, T. Kim, H. Chung, H. Jang, J. Lee, D. Kim, E. Jang, Nature **575**, 634 (2019). https://doi.org/10.1038/s41586-019-1771-5
19. T. Kim, K.H. Kim, S. Kim, S.M. Choi, H. Jang, H.K. Seo, H. Lee, D.Y. Chung, E. Jang, Nature **586**, 385 (2020). https://doi.org/10.1038/s41586-020-2791-x
20. K. Lee, Y. Kim, E. Ahn, J.I. Kwon, H. Ma, J.H. Jang, S. Li, H.C. Lee, G. Heon Lee, S. Lee, K. Kim, N.J. Sung, D. Kim, M.H. Song, M.K. Choi, J. Yang, Mater. Today (2024). https://doi.org/10.1016/j.mattod.2024.03.008
21. H. Xu, J. Song, P. Zhou, Y. Song, J. Xu, H. Shen, S. Fang, Y. Gao, Z. Zuo, J.M. Pina, O. Voznyy, C. Yang, Y. Hu, J. Li, J. Du, E.H. Sargent, F. Fan, Nat. Photon. **18**, 186 (2024). https://doi.org/10.1038/s41566-023-01344-4
22. S.-Y. Yoon, Y.-J. Lee, H. Yang, D.-Y. Jo, H.-M. Kim, Y. Kim, S.M. Park, S. Park, H. Yang, ACS Energy Lett. **7**, 2247 (2022). https://doi.org/10.1021/acsenergylett.2c01065
23. W.K. Bae, J. Lim, Korean J. Chem. Eng. **36**, 173 (2019). https://doi.org/10.1007/s11814-018-0193-7
24. G.H. Lee, K. Kim, Y. Kim, J. Yang, M.K. Choi, Nano-Micro Lett. **16**, 45 (2024). https://doi.org/10.1007/s40820-023-01254-8
25. C. Xue, Y. Ni, X. Zhao, N. He, J. Li, H. Yu, M. Zhang, X. Liu, B. Wang, J. Sun, X. Han, J. Zhang, J. Sun, Y. Tong, Q. Tang, Y. Liu, Mater. Today Phys. **36**, 101157 (2023). https://doi.org/10.1016/j.mtphys.2023.101157
26. J.J. Kim, Y. Wang, H. Wang, S. Lee, T. Yokota, T. Someya, Adv. Funct. Mater. **31**, 2009602 (2021). https://doi.org/10.1002/adfm.202009602
27. C. Bai, K. Ji, H. Wang, J. Zhang, G. Hu, D. Kong, A.C.S. Mater, Lett. **4**, 2401 (2022). https://doi.org/10.1021/acsmaterialslett.2c00743
28. J.C. Yang, J. Mun, S.Y. Kwon, S. Park, Z. Bao, S. Park, Adv. Mater. **31**, 1904765 (2019). https://doi.org/10.1002/adma.201904765
29. Y. Jeon, H.R. Choi, J.H. Kwon, S. Choi, K.M. Nam, K.C. Park, K.C. Choi, Light Sci. Appl. **8**, 114 (2019). https://doi.org/10.1038/s41377-019-0221-3
30. J. Choi, I.S. Lee, J.S. Lee, S. Jeon, W.S. Yun, S. Yang, Y. Moon, J. Kim, J. Kim, S. Choy, C. Jeong, M.K. Shim, T.-I. Kim, and K. Kim Biomaterials Research **26**, 56 (2022). https://doi.org/10.1186/s40824-022-00305-2
31. Y. Lee, J. Park, A. Choe, S. Cho, J. Kim, H. Ko, Adv. Funct. Mater. **30**, 1904523 (2020). https://doi.org/10.1002/adfm.201904523
32. J.H. Jang, S. Li, D.-H. Kim, J. Yang, M.K. Choi, Adv. Elec. Mater. **9**, 2201271 (2023). https://doi.org/10.1002/aelm.202201271
33. K. Kim, B. Kim, C.H. Lee, Adv. Mater. **32**, 1902051 (2020). https://doi.org/10.1002/adma.201902051
34. M.K. Choi, J. Yang, K. Kang, D.C. Kim, C. Choi, C. Park, S.J. Kim, S.I. Chae, T.H. Kim, J.H. Kim, T. Hyeon, D.-H. Kim, Nat. Commun. **6**, 7149 (2015). https://doi.org/10.1038/ncomms8149
35. S. Nam, C. Park, S.H. Sunwoo, M. Kim, H. Lee, M. Lee, D.-H. Kim, Soft Sci. **3**, 28 (2023). https://doi.org/10.20517/ss.2023.19
36. G. Macrelli, A.K. Varshneya, J.C. Mauro, Opt. Mater. **106**, 109994 (2020). https://doi.org/10.1016/j.optmat.2020.109994
37. Y. Yuan, Y. Yalikun, S. Amaya, Y. Aishan, Y. Shen, Y. Tanaka, Sens. Actuators A **321**, 112604 (2021). https://doi.org/10.1016/j.sna.2021.112604
38. J. Shi, D. Ma, G.F. Han, Y. Zhang, Q. Ji, T. Gao, J. Sun, X. Song, C. Li, Y. Zhang, X.Y. Lang, Y. Zhang, Z. Liu, ACS Nano **8**, 10196 (2014). https://doi.org/10.1021/nn503211t
39. Z. You, H. Liu, Y. Xu, Z. Ma, G. Qin, J. Phys. D Appl. Phys. **54**, 11LT01 (2021). https://doi.org/10.1088/1361-6463/abd05f
40. X. Yang, E. Multlugun, C. Dang, K. Dev, Y. Gao, S.T. Tan, X.W. Sun, H.V. Demir, ACS Nano **8**, 8224 (2014). https://doi.org/10.1021/nn502588k
41. T. Agag, T. Koga, T. Takeichi, Polymer **42**, 3399 (2001). https://doi.org/10.1016/S0032-3861(00)00824-7
42. Y. Hishiyama, S. Yasuda, A. Yoshida, M. Inagaki, J. Mater. Sci. **23**, 3272 (1988). https://doi.org/10.1007/BF00551305
43. J. Su, A.C. Lua, J. Memb. Sci. **305**, 263 (2007). https://doi.org/10.1016/j.memsci.2007.08.010
44. J.A. Cella, Polym. Degrad. Stab. **36**, 99 (1992). https://doi.org/10.3390/nano8070517
45. Q. Su, H. Zhang, S. Chen, npj Flex Electron. **5**, 8 (2021). https://doi.org/10.1038/s41528-021-00106-y
46. D.W. Shin, Y.H. Suh, S. Lee, B. Hou, S.D. Han, Y. Cho, X.B. Fan, S.Y. Bang, S. Zhan, J. Yang, H.W. Choi, S. Jung, F.C. Mocanu, H. Lee, L. Occhipinti, Y.T. Chun, G. Amaratunga, J.M. Kim, Adv. Opt. Mater. **8**, 1901362 (2020). https://doi.org/10.1002/adom.201901362
47. H. Seung, C. Choi, D.C. Kim, J.S. Kim, J.H. Kim, J. Kim, S.I. Park, J.A. Lim, J. Yang, M.K. Choi, T. Hyeon, D.-H. Kim, Sci. Adv. **8**, eabq3101 (2022). https://doi.org/10.1126/sciadv.abq3101
48. F. Li, J. Shen, X. Liu, Z. Cao, X. Cai, J. Li, K. Ding, J. Liu, G. Tu, Org. Electron. **51**, 54 (2017). https://doi.org/10.1016/j.orgel.2017.09.010
49. X. Yu, Z. Zhu, X. Wu, G. Li, R. Cheng, R. Qing, Q. Li, S. Chen, Nanoscale **12**, 19953 (2020). https://doi.org/10.1039/d0nr04676k

50. R. Wang, Q. Yuan, Z. Kang, R. Wang, D. Zhang, W. Ji, Flex. Print. Electron **7**, 015006 (2022). https://doi.org/10.1088/2058-8585/ac4e67
51. G.W. Baek, H. Seo, T. Lee, D. Hahm, W.K. Bae, J. Kwak, J. Flex. Print. Electron **2**, 243 (2023). https://doi.org/10.56767/jfpe.2023.2.2.243
52. Y.T. Li, D.T. Chen, C.F. Han, J.F. Lin, Vacuum **183**, 109844 (2021). https://doi.org/10.1016/j.vacuum.2020.109844
53. K. Zeng, F. Zhu, J. Hu, L. Shen, K. Zhang, H. Gong, Thin Solid Films **443**, 60 (2003). https://doi.org/10.1016/S0040-6090(03)00915-5
54. C. Hengst, S.B. Menzel, G.K. Rane, V. Smirnov, K. Wilken, B. Leszczynska, D. Fischer, N. Prager, Materials **10**, 245 (2017). https://doi.org/10.3390/ma10030245
55. T.D. Jung, P.K. Song, Curr. Appl. Phys. **11**, S314 (2011). https://doi.org/10.1016/j.cap.2011.03.042
56. S. Kim, H.W. Cho, K. Hong, J.H. Son, K. Kim, B. Koo, S. Kim, J.L. Lee, Opt. Express **22**, A1257 (2014). https://doi.org/10.1364/OE.22.0A1257
57. C. Guillén, J. Herrero, Sol. Energy Mater. Sol. Cells **92**, 938 (2008). https://doi.org/10.1016/j.solmat.2008.02.038
58. S.J. Oh, S. Lee, K.C. Choi, J.H. Kwon, T.S. Kim, J. Mater. Chem. C **11**, 7262 (2023). https://doi.org/10.1039/d3tc01002c
59. Z. Wang, S. Wang, J. Wang, Y. Niu, X. Zong, C. Li, S. Jiang, H. Zhao, Ceram. Int. **47**, 31442 (2021). https://doi.org/10.1016/j.ceramint.2021.08.020
60. S.H. Park, S.M. Lee, E.H. Ko, T.H. Kim, Y.C. Nah, S.J. Lee, J.H. Lee, H.K. Kim, Sci. Rep. **6**, 33868 (2016). https://doi.org/10.1038/srep33868
61. X. Tang, Z. Hu, Z. Wang, J. Chen, X. Mu, G. Song, P. Sun, Z. Wen, J. Hao, S. Cong, Z. Zhao, eScience. **2**, 632 (2022). https://doi.org/10.1016/j.esci.2022.08.005
62. J.K. Song, D. Son, J. Kim, Y.J. Yoo, G.J. Lee, L. Wang, M.K. Choi, J. Yang, M. Lee, K. Do, J.H. Koo, N. Lu, J.H. Kim, T. Hyeon, Y.M. Song, D.-H. Kim, Adv. Funct. Mater. **27**, 1605286 (2017). https://doi.org/10.1002/adfm.201605286
63. J. Lee, K. Hyun, Y. Kwon, Korean J. Chem. Eng. **40**, 1775 (2023). https://doi.org/10.1007/s11814-023-1409-z
64. M.K. Choi, I. Park, D.C. Kim, E. Joh, O.K. Park, J. Kim, M. Kim, C. Choi, J. Yang, K.W. Cho, J.H. Hwang, J.M. Nam, T. Hyeon, J.H. Kim, D.-H. Kim, Adv. Funct. Mater. **25**, 7109 (2015). https://doi.org/10.1002/adfm.201502956
65. C. Ji, D. Liu, C. Zhang, L. JayGuo, Nat. Commun. **11**, 3367 (2020). https://doi.org/10.1038/s41467-020-17107-6
66. K. Hong, J.H. Son, S. Kim, B.H. Koo, J.L. Lee, Chem. Commun. **48**, 10606 (2012). https://doi.org/10.1039/c2cc35713e
67. H. Najafi-Ashtiani, B. Akhavan, F. Jing, M.M. Bilek, ACS Appl. Mater. Interfaces **11**, 14871 (2019). https://doi.org/10.1021/acsami.9b00191
68. M. Kim, D. Kim, O. Kwon, H. Lee, Micromachines **13**, 269 (2022). https://doi.org/10.3390/mi13020269
69. S. Lee, J. Kim, H. Lee, Nanomaterials **13**, 1780 (2023). https://doi.org/10.3390/nano13111780
70. H.H. Kim, K. Kim, J. Yang, M.K. Choi, Adv. Mater. Technol. **9**, 2301262 (2024). https://doi.org/10.1002/admt.202301262
71. K. Zhang, L. Meng, M. Zhang, Y. Li, L. Jiang, H. Liu, Adv. Funct. Mater. **34**, 2308468 (2023). https://doi.org/10.1002/adfm.202308468
72. C. Zhang, Q. Huang, Q. Cui, C. Ji, Z. Zhang, X. Chen, T. George, S. Zhao, L.J. Guo, A.C.S. Appl, Mater. Interfaces. **11**, 27216 (2019). https://doi.org/10.1021/acsami.9b08289
73. K. Ding, Y. Fang, S. Dong, H. Chen, B. Luo, K. Jiang, H. Gu, L. Fan, S. Liu, B. Hu, L. Wang, Adv. Opt. Mater. **6**, 1800347 (2018). https://doi.org/10.1002/adom.201800347
74. M. Kaltenbrunner, M.S. White, E.D. Głowacki, T. Sekitani, T. Someya, N.S. Sariciftci, S. Bauer, Nat. Commun. **3**, 770 (2012). https://doi.org/10.1038/ncomms1772
75. S. Choi, H. Lee, R. Ghaffari, T. Hyeon, D.-H. Kim, Adv. Mater. **28**, 4203 (2016). https://doi.org/10.1002/adma.201504150
76. J.I. Kwon, G. Park, G.H. Lee, J.H. Jang, N.J. Sung, S.Y. Kim, J. Yoo, K. Lee, H. Ma, M. Karl, T.J. Shin, M.H. Song, J. Yang, M.K. Choi, Sci. Adv. **8**, 0697 (2022). https://doi.org/10.1126/sciadv.add0697
77. J.M. Caruge, J.E. Halpert, V. Wood, V. Buloví, M.G. Bawendi, Nat. Photonics **2**, 247 (2008). https://doi.org/10.1038/nphoton.2008.34
78. P.O. Anikeeva, J.E. Halpert, M.G. Bawendi, V. Bulović, Nano Lett. **7**, 2196 (2007). https://doi.org/10.1021/nl0703424
79. M.K. Choi, J. Yang, D.C. Kim, Z. Dai, J. Kim, H. Seung, V.S. Kale, S.J. Sung, C.R. Park, N. Lu, T. Hyeon, D.-H. Kim, Adv. Mater. **30**, 1703279 (2018). https://doi.org/10.1002/adma.201703279
80. J. Geng, Adv. Opt. Photonics. **5**, 456 (2013). https://doi.org/10.1364/AOP.5.000456
81. H. Zhang, J. Paik, Adv. Funct. Mater. **32**, 2107401 (2022). https://doi.org/10.1002/adfm.202107401
82. Y. Tang, Y. Li, Y. Hong, S. Yang, J. Yin, Proc. Natl. Acad. Sci. U. S. A. **116**, 26407 (2019). https://doi.org/10.1073/pnas.1906435116
83. T. van Manen, S. Janbaz, M. Ganjian, A.A. Zadpoor, Mater. Today **32**, 59 (2020). https://doi.org/10.1016/j.mattod.2019.08.001
84. Q. Zhang, J. Wommer, C. O'Rourke, J. Teitelman, Y. Tang, J. Robison, G. Lin, J. Yin, Extrem. Mech. Lett. **11**, 111 (2017). https://doi.org/10.1016/j.eml.2016.08.004
85. T. Kim, J.S. Price, A. Grede, S. Lee, G. Choi, W. Guan, T.N. Jackson, N.C. Giebink, Adv. Mater. Technol. **3**, 1800067 (2018). https://doi.org/10.1002/admt.201800067
86. D.C. Kim, H. Yun, J. Kim, H. Seung, W.S. Yu, J.H. Koo, J. Yang, J.H. Kim, T. Hyeon, D.-H. Kim, Nat. Electron. **4**, 671 (2021). https://doi.org/10.1038/s41928-021-00643-4
87. J. Kim, H.J. Shim, J. Yang, M.K. Choi, D.C. Kim, J. Kim, T. Hyeon, D.-H. Kim, Adv. Mater. **29**, 1700217 (2017). https://doi.org/10.1002/adma.201700217
88. K. Zhang, Y.H. Jung, S. Mikael, J.H. Seo, M. Kim, H. Mi, H. Zhou, Z. Xia, W. Zhou, S. Gong, Z. Ma, Nat. Commun. **8**, 1782 (2017). https://doi.org/10.1038/s41467-017-01926-1
89. H. Fu, K. Nan, W. Bai, W. Huang, K. Bai, L. Lu, C. Zhou, Y. Liu, F. Liu, J. Wang, M. Han, Z. Yan, H. Luan, Y. Zhang, Y. Zhang, J. Zhao, X. Cheng, M. Li, J.W. Lee, Y. Liu, D. Fang, X. Li, Y. Huang, Y. Zhang, J.A. Rogers, Nat. Mater. **17**, 268 (2018). https://doi.org/10.1038/s41563-017-0011-3
90. Y. Lee, B.J. Kim, L. Hu, J. Hong, J.H. Ahn, Mater. Today **53**, 51 (2022). https://doi.org/10.1016/j.mattod.2022.01.017
91. B. Jang, S. Won, J. Kim, J. Kim, M. Oh, H.J. Lee, J.H. Kim, Adv. Funct. Mater. **32**, 2113299 (2022). https://doi.org/10.1002/adfm.202113299
92. Y. Lee, D.S. Kim, S.W. Jin, H. Lee, Y.R. Jeong, I. You, G. Zi, J.S. Ha, Chem. Eng. J. **427**, 130858 (2022). https://doi.org/10.1016/j.cej.2021.130858
93. H. Shi, C. Liu, Q. Jiang, J. Xu, Adv. Electron. Mater. **1**, 1500017 (2015). https://doi.org/10.1002/aelm.201500017
94. X. Fan, J. Wang, H. Wang, X. Liu, H. Wang, A.C.S. Appl, Mater. Interfaces **7**, 16287 (2015). https://doi.org/10.1021/acsami.5b02830
95. A.A. Jan, S. Kim, S. Kim, Soft Sci. **4**, 10 (2024). https://doi.org/10.20517/ss.2023.54
96. K. Lee, D. Kim, J. Shim, S. Bae, D.J. Shin, B.E. Treml, J. Yoo, T. Hanrath, W.D. Kim, D.C. Lee, Combust. Flame **162**, 3823 (2015). https://doi.org/10.1016/j.combustflame.2015.07.019

97. Y. Wang, Y. Qiu, S.K. Ameri, H. Jang, Z. Dai, Y.A. Huang, N. Lu, npj Flex Electron. **2**, 6 (2018). https://doi.org/10.1038/s41528-017-0019-4
98. N. Lu, S. Yang, Curr. Opin. Solid State Mater. Sci. **19**, 149 (2015). https://doi.org/10.1016/j.cossms.2014.12.007
99. K.Y. Lai, S. Yang, P.R. Chen, M.H. Yeh, M.L. Liao, C.W. Yeh, S.J. Ho, Y.T. Chang, H.S. Chen, Adv. Mater. Technol. **7**, 2100889 (2022). https://doi.org/10.1002/admt.202100889
100. N. Kim, J. Kim, J. Seo, C. Hong, J. Lee, A.C.S. Appl, Mater. Interfaces **14**, 4344 (2022). https://doi.org/10.1021/acsami.1c23160
101. Y. Lee, G. Jung, S.W. Jin, J.S. Ha, A.C.S. Appl, Mater. Interfaces **14**, 48844 (2022). https://doi.org/10.1021/acsami.2c13277
102. S.H. Kim, G.W. Baek, J. Yoon, S. Seo, J. Park, D. Hahm, J.H. Chang, D. Seong, H. Seo, S. Oh, K. Kim, H. Jung, Y. Oh, H.W. Baac, B. Alimkhanuly, W.K. Bae, S. Lee, M. Lee, J. Kwak, J.H. Park, D. Son, Adv. Mater. **33**, 2104690 (2021). https://doi.org/10.1002/adma.202104690
103. S. Ju, Y. Zhu, H. Hu, Y. Liu, Z. Xu, J. Zheng, C. Mao, Y. Yu, K. Yang, L. Lin, T. Guo, F. Li, Light Sci. Appl. **11**, 331 (2022). https://doi.org/10.1038/s41377-022-01036-8
104. B. Lee, J.Y. Oh, H. Cho, C.W. Joo, H. Yoon, S. Jeong, E. Oh, J. Byun, H. Kim, S. Lee, J. Seo, C.W. Park, S. Choi, N.M. Park, S.Y. Kang, C.S. Hwang, S.D. Ahn, J.I. Lee, Y. Hong, Nat. Commun. **11**, 663 (2020). https://doi.org/10.1038/s41467-020-14485-9
105. G.D. Cha, D.-H. Kim, D.C. Kim, Korean J. Chem. Eng. **41**, 1 (2024). https://doi.org/10.1007/s11814-023-00006-z
106. H. Chen, J. He, R. Lanzafame, I. Stadler, H. El Hamidi, H. Liu, J. Celli, M.R. Hamblin, Y. Huang, E. Oakley, G. Shafirstein, H.K. Chung, S.T. Wu, Y. Dong, J. Soc. Inf. Disp. **25**, 177 (2017). https://doi.org/10.1002/jsid.543
107. S. Patel, F. Ershad, M. Zhao, R.R. Isseroff, B. Duan, Y. Zhou, Y. Wang, C. Yu, Soft Sci. **2**, 9 (2022). https://doi.org/10.20517/ss.2022.13
108. D. Pollreisz, N. TaheriNejad, Mob. Networks Appl. **27**, 728 (2022). https://doi.org/10.1007/s11036-019-01323-6
109. P.M. Mohan, A.A. Nisha, V. Nagarajan, E.S.J. Jothi, Int. Conf. Commun. Signal. Process. (2016). https://doi.org/10.1109/ICCSP.2016.7754330
110. S. Li, J.H. Jang, W. Chung, H. Seung, S.I. Park, H. Ma, W.J. Pyo, C. Choi, D.S. Chung, D.-H. Kim, M.K. Choi, J. Yang, ACS Nano **17**, 20013 (2023). https://doi.org/10.1021/acsnano.3c05178
111. T.H. Kim, C.S. Lee, S. Kim, J. Hur, S. Lee, K.W. Shin, Y.Z. Yoon, M.K. Choi, J. Yang, D.-H. Kim, T. Hyeon, S. Park, S. Hwang, ACS Nano **11**, 5992 (2017). https://doi.org/10.1021/acsnano.7b01894
112. J. Přibil, A. Přibilová, I. Frollo, Eng. Proc. **2**, 69 (2020). https://doi.org/10.3390/ecsa-7-08204
113. H.S. Lee, B. Noh, S.U. Kong, Y.H. Hwang, H.E. Cho, Y. Jeon, K.C. Choi, Npj Flex. Electron. **7**, 15 (2023). https://doi.org/10.1038/s41528-023-00248-1
114. E.F. Pribadi, R.K. Pandey, P.C.P. Chao, Microsyst. Technol. **26**, 3409 (2020). https://doi.org/10.1007/s00542-020-04895-6
115. E.F. Pribadi, R.K. Pandey, P.C.P. Chao, Microsyst. Technol. **27**, 2461 (2021). https://doi.org/10.1007/s00542-020-05154-4
116. W. Liu, C. Zhang, R. Alessandri, B.T. Diroll, Y. Li, H. Liang, X. Fan, K. Wang, H. Cho, Y. Liu, Y. Dai, Q. Su, N. Li, S. Li, S. Wai, Q. Li, S. Shao, L. Wang, J. Xu, X. Zhang, D.V. Talapin, J.J. de Pablo, S. Wang, Nat. Mater. **22**, 737 (2023). https://doi.org/10.1038/s41563-023-01529-w
117. M.W. Jeong, J.H. Ma, J.S. Shin, J.S. Kim, G. Ma, T.U. Nam, X. Gu, S.J. Kang, J.Y. Oh, Sci. Adv. **9**, 1504 (2023). https://doi.org/10.1126/sciadv.adh1504
118. J.H. Kim, J.W. Park, Sci. Adv. **7**, eabd9715 (2021). https://doi.org/10.1126/sciadv.abd9715
119. J. Yoo, S. Ha, G.H. Lee, Y. Kim, M.K. Choi, Adv. Funct. Mater. **33**, 2302473 (2023). https://doi.org/10.1002/adfm.202302473
120. S. Oh, S. Lee, S.-H. Byun, S. Lee, C.Y. Kim, J. Yea, S. Chung, S. Li, K.-I. Jang, J. Kang, J.-W. Jeong, Adv. Funct. Mater. **33**, 2214766 (2023). https://doi.org/10.1002/adfm.202214766
121. D.C. Kim, H. Seung, J. Yoo, J. Kim, H.H. Song, J.S. Kim, Y. Kim, K. Lee, C. Choi, D. Jung, C. Park, H. Heo, J. Yang, T. Hyeon, M.K. Choi, D.H. Kim, Nat. Electron. (2024). https://doi.org/10.1038/s41928-024-01152-w
122. J.H. Yu, J. Kim, T. Hyeon, J. Yang, J. Chem. Phys. **151**, 244701 (2019). https://doi.org/10.1063/1.5128511
123. J.-Y. Kim, J. Yang, J.H. Yu, W. Baek, C.-H. Lee, H.J. Son, T. Hyeon, M.J. Ko, ACS Nano **9**, 11286 (2015). https://doi.org/10.1021/acsnano.5b04917
124. Y. Choi, D. Kim, Y.S. Shin, W. Lee, S. Orr, J.Y. Kim, J. Park Nanoscale **14**, 2771 (2022). https://doi.org/10.1039/D1NR08038E
125. B.G. Jeong, J.H. Chang, D. Hahm, S. Rhee, M. Park, S. Lee, Y. Kim, D. Shin, J.W. Park, C. Lee, D.C. Lee, K. Park, E. Hwang, W.K. Bae, Nat. Mater. **21**, 246 (2022). https://doi.org/10.1038/s41563-021-01119-8
126. H.J. Lee, S. Im, D. Jung, K. Kim, J.A. Chae, J. Lim, J.W. Park, D. Shin, K. Char, B.G. Jeong, J.-S. Park, E. Hwang, D.C. Lee, Y.-S. Park, H.-J. Song, J.H. Chang, W.K. Bae, Nat. Commun. **14**, 3779 (2023). https://doi.org/10.1038/s41467-023-39509-y
127. S. Li, S.M. Jung, W. Chung, J.W. Seo, H. Kim, S.I. Park, H.C. Lee, J.S. Han, S.B. Ha, I.Y. Kim, S.I. In, J.Y. Kim, and. J. Yang Carbon Energy. **5**, e384 (2023). https://doi.org/10.1002/cey2.384
128. Y. Choi, D. Hahm, W.K. Bae, J. Lim, J. Nat. Commun. **14**, 43 (2023). https://doi.org/10.1038/s41467-022-35731-2
129. L.J. Lim, X. Zhao, Z.K. Tan, Adv. Mater. **35**, 2301887 (2023). https://doi.org/10.1002/adma.202301887
130. K. Kim, D. Hahm, G.W. Baek, T. Lee, D. Shin, J. Lim, W.K. Bae, J. Kwak ACS Appl. Electron. Mater. **4**, 6229 (2022). https://doi.org/10.1021/acsaelm.2c01351
131. H. Ma, D. Kim, S.I. Park, B.K. Choi, G. Park, H. Baek, H. Lee, H. Kim, J.S. Yu, W.C. Lee, J. Park, J. Yang, Adv. Sci. **10**, 2205690 (2023). https://doi.org/10.1002/advs.202205690
132. J. Zhang, J. Li, Z. Ye, J. Cui, X. Peng, J. Am. Chem. Soc. **145**, 13938 (2023). https://doi.org/10.1021/jacs.3c03443
133. H. Ma, S. Kang, S. Lee, G. Park, Y. Bae, G. Park, J. Kim, S. Li, H. Baek, H. Kim, J.S. Yu, H. Lee, J. Park, J. Yang, ACS Nano **17**, 13734 (2023). https://doi.org/10.1021/acsnano.3c03103
134. J. Yang, J. Yoo, W.S. Yu, M.K. Choi, Macromol. Res. **29**, 391 (2021). https://doi.org/10.1007/s13233-021-9055-y
135. D. Hahm, J. Lim, H. Kim, J.-W. Shin, S. Hwang, S. Rhee, J.H. Chang, J. Yang, C.H. Lim, H. Jo, B. Choi, N.S. Cho, Y.-S. Park, D.C. Lee, E. Hwang, S. Chung, C.-M. Kang, M.S. Kang, W.K. Bae, Nat. Nanotechnol. **17**, 952 (2022). https://doi.org/10.1038/s41565-022-01182-5
136. H. Park, C. Na, H. Lee, S.M. Cho, Korean J. Chem. Eng. **40**, 667 (2023). https://doi.org/10.1007/s11814-022-1255-4
137. S.Y. Kim, J.I. Kwon, H.H. Song, G.H. Lee, W.S. Yu, S. Li, M.K. Choi, J. Yang, Appl. Surf. Sci. **610**, 155579 (2023). https://doi.org/10.1016/j.apsusc.2022.155579
138. S.Y. Park, S. Lee, J. Yang, M.S. Kang, Adv. Mater. **35**, 230056 (2023). https://doi.org/10.1002/adma.202300546
139. J. Lee, J. Ha, H. Lee, H. Cho, D.C. Lee, D.V. Talapin, H. Cho, ACS Energy Lett. **8**, 4210 (2023). https://doi.org/10.1021/acsenergylett.3c01019
140. S.H. Noh, W.J. Jeong, K.H. Lee, H.S. Yang, E.H. Suh, J. Jung, S.C. Park, D. Lee, I.H. Jung, Y.J. Jeong, J. Jang Adv. Funct. Mater. **33**, 2304004 (2023). https://doi.org/10.1002/adfm.202304004

141. J.Y. Lee, E.A. Kim, Y. Choi, J. Han, D. Hahm, D. Shin, W.K. Bae, J. Lim, S.-Y. Cho, ACS Photonics **10**, 2598 (2023). https://doi.org/10.1021/acsphotonics.3c00332